Ultrasonics 93 (2019) 122–129

Contents lists available at ScienceDirect

Ultrasonics

journal homepage: www.elsevier.com/locate/ultras

Amplitude modified sparse imaging for damage detection in quasi-isotropic composite laminates using non-contact laser induced Lamb waves

Fei Gao[a], Jiadong Hua[b], Liang Zeng[a], Jing Lin[c,*]

[a] Shaanxi Key Laboratory of Mechanical Product Quality Assurance and Diagnostics, School of Mechanical Engineering, Xi'an Jiaotong University, Xi'an, Shaanxi Province 710049, China

[b] School of Reliability and Systems Engineering, Beihang University, Xueyuan Road No. 37, Haidian District, Beijing, China

[c] Science & Technology on Reliability and Environmental Engineering Laboratory, School of Reliability and Systems Engineering, Beihang University, Xueyuan Road No. 37, Haidian District, Beijing, China

ARTICLE INFO

Keywords:
Lamb waves
Composite laminates
Laser induced Lamb wave
Amplitude modified dictionary
Sparse imaging

ABSTRACT

Composite structure is increasingly used in civil and aerospace applications due to its high mechanical performance. Lamb wave based sparse reconstruction imaging for damage localization is promising for structural health monitoring (SHM) and nondestructive evaluation (NDE) by using few measurements. However, this dictionary based method requires accurate atoms to represent Lamb wave propagating features in structure very well. Besides dispersion, signal changes caused by amplitude modulation should be considered for waveform distortion when constructing the dictionary for sparse imaging method. In this paper, a non-contact laser is used for Lamb wave excitation which exhibits a strong amplitude modulation in low frequency. Additionally, the strong attenuation resulting from material damping would also presents a distance-dependent amplitude modulation. To reconstruct an amplitude model of Lamb wave, the decomposition method of system response and attenuation is proposed. Then, the influence of amplitude modulation on signal representation is analyzed, which shows the restriction of dictionary without considering amplitude modulation. On this basis, the amplitude considered dictionary is built together with the phase considered dictionary for sparse imaging in terms of damage detection. Furthermore, according to Lamb wave reflection model, the solution for sparse reconstruction imaging is given. Finally, the performance of sparse imaging method is discussed by experimental investigation with different parameters. The results show the efficiency of the proposed method with improved imaging performance and give comparisons for better parameter choice.

1. Introduction

Advanced composite structures are increasingly used in aerospace and civil applications due to their high strength-to-weight ratio, excellent corrosion resistance and outstanding design ability [1]. However, damages (e.g. delamination, fiber breaking and matrix crack) induced by sudden impact or lighting strike will cause the material strength degrading which may finally result in catastrophic failures [2]. Lamb wave based nondestructive evaluation (NDE) and structure health monitoring (SHM) are promising ways to monitor the structural health because Lamb waves are sensitive to both surface and sub-surface damages in composite laminates [3]. Meanwhile, Lamb waves can propagate over long distances with high speed, which means a higher efficiency compared with traditional ultrasonic methods [4,5].

Lamb waves can be generated by PZT [6], electromagnetic acoustic transducers (EMATs) [7], laser sources [8] and so on. Among them, the laser source is commonly used due to the advantages including non-contact broadband excitation, relative high pulse energy, and high spatial resolution [9,10]. Besides the multimodal and dispersive natures of Lamb waves, the amplitude modulation (including mode tuning, source and transducer response, attenuation, etc.) will also change the appearance of the response signals [11]. Especially by using non-contact laser source as actuators, the strong amplitude modulation in low frequency will increase signal interpreting difficulties.

The general configuration of Lamb wave based detection method is using sparse source - sensor pairs to capture damage features. Various imaging algorithms can be used to locate the possible damages like delay-and-sum (DAS) method [12], iterative algebraic reconstruction technique (ART) [13] and probability-based Diagnostic Imaging (PDI) [14]. Compared with those methods, another promising technique called sparse imaging is developed which is based on the sparsity assumption of damages existed in the structure. The theory behind sparse

* Corresponding author.
E-mail addresses: gf.4992328@stu.xjtu.edu.cn (F. Gao), huajiadong@buaa.edu.cn (J. Hua), liangzeng@mail.xjtu.edu.cn (L. Zeng), linjing@buaa.edu.cn (J. Lin).

https://doi.org/10.1016/j.ultras.2018.10.008
Received 10 July 2018; Received in revised form 20 September 2018; Accepted 19 October 2018
Available online 21 October 2018
0041-624X/

imaging method is using over-completed dictionaries to match the response signals, which provides a high resolution detection results [15]. Typically, Mallat and Zhang [16] proposed a matching pursuits method to represent the signals with dictionary of Gabor function. Levine and Michaels [17] compared three different sparse reconstruction methods (i.e. basis pursuit denoising, orthogonal matching pursuit and hybrid reconstruction method) for damage detection on an aluminum plate, the accurate results shows the efficiency of these methods. Marchi et al. [18] presents a warped frequency transform based basis pursuit algorithm to represent broadband multimodal Lamb waves which shows efficiency for the analysis of multimodal and dispersive Lamb waves. However, most of foregoing studies build dictionaries without taking amplitude modulation into consideration. Only the phase information coming from dispersion relation is used. However, for laser induced Lamb waves in composite structures, the strong amplitude modulation will affect the accuracy of dictionaries.

In order to address the above issues, in this paper, the amplitude modulation and the phase information are both considered for dictionary construction so as to make the atoms in dictionary more consistent with the raw signal. Firstly, the amplitude modulation is decomposed into distance-dependent attenuation and system response. Then, the comparison of simulated signals with and without considering amplitude modulation shows the necessity of amplitude consideration for signal matching process. Using amplitude information captured through experimental studies, the amplitude modified dictionary is constructed, which is further adopted for sparse reconstruction imaging. Finally, the algorithm performance is also discussed by changing the denoising parameter and the number of sources.

This paper is organized as follows. The background of laser induced Lamb waves is reviewed in Section 2. The amplitude decomposition method and the analysis of waveform distortion caused by amplitude modulation are given in Section 3. In Section 4, the amplitude modified dictionary is designed in frequency domain and the solution for sparse imaging is also presented. Experiment validation is carried out on a CFRP plate using non-contact laser excitation in Section 5. Conclusions are given in Section 6.

2. Review of laser induced Lamb waves

2.1. Lamb waves theory

Lamb waves are one kind of elastic waves propagating in solid plates with free boundaries. Based on Rayleigh-Lamb equation [19], two families of Lamb wave mode can be solved (i.e. symmetric modes and antisymmetric modes). Additionally, each mode of Lamb wave is dispersive, which means both phase velocity and group velocity for a single wave mode are frequency dependent.

The governing equations for Lamb wave solution in isotropic plates are given as follows

$$\begin{aligned} &\frac{\tan(qh)}{\tan(ph)} = -\frac{4k^2qp}{(k^2-q^2)^2} \quad \text{for symmetric modes (S modes),} \\ &\frac{\tan(qh)}{\tan(ph)} = -\frac{(k^2-q^2)^2}{4k^2qp} \quad \text{for anti} \\ &\qquad - \text{symmetric modes (A modes),} \end{aligned} \tag{1}$$

where p and q are given by

$$p^2 = \left(\frac{\omega}{C_L}\right)^2 - k^2, \quad q^2 = \left(\frac{\omega}{C_T}\right)^2 - k^2, \tag{2}$$

where C_L and C_T are the velocities of longitudinal and transverse waves, respectively. The thickness of the plate is $2h$ and k is the wave number that equals to ω/c_{phase}. The $k(\omega)$ solved by Eq. (1) for k and ω are called dispersion curves, which provide the information for dispersion and multi-modes. Basically, there are at least two modes of Lamb waves can exist in any frequency range theoretically.

Table 1
Material properties of the CFRP plate.

Material	E_1 (GPa)	E_2 (GPa)	G_{12} (GPa)	ν_{12}	ν_{23}	ρ (kg/m^3)
CFRP	135	10.9	4.7	0.285	0.4	1560

For plates with various layers, the material property and anisotropy for each layer should be considered. The most general method for solving the dispersion curves of Lamb waves in anisotropic laminates is using partial wave technique [20]. As the boundary conditions for the whole laminates are still free boundaries, by employing transfer matrix or global matrix methods [21], the dispersion curves $k(\omega)$ for laminates can be solved with a pre-knowledge of laminates. The composite material properties for the single layer used in this paper are given in Table 1. Hence, the dispersion relations can be calculated.

2.2. Laser source excitation and narrowband extraction

The typical characters for Lamb wave propagation are multi-mode, dispersion and amplitude modulation, which may distort the waveforms when compared with the excitation waveforms. Assuming that the excitation signal is $s(t)$ and ignoring mode conversion, for mode m, the response of signal $g^m(t)$ with a propagation distance of d can be represented as [22]

$$g^m(t) = \int A^m(\omega)S(\omega)\exp[ik^m(\omega)d]\exp(-\alpha(\omega)d)\exp(-i\omega t)d\omega, \tag{3}$$

where $A(\omega)$ is system response including laser source thermoelastic coefficient, sensor mechanical-electro coefficient, equipmental modulation and mode excitability, which is distance independent. $\alpha(\omega)$ is frequency dependent attenuation coefficient, which is related to material damping. $k^m(\omega)$ is the dispersion curve for mode m and $S(\omega)$ is the Fourier transform of $s(t)$.

For non-contact sources, laser source is commonly used under the theory of thermoelastic effect [23]. That is, when a solid is illuminated by a laser source, the localized increased temperature will cause a sudden thermal expansion and then generate ultrasonic waves. Laser induced waves are generally broadband in frequency with narrow time duration, like a pulse waveform shape [24]. The example signal using Nd: YAG laser source and PZT receiver is given in Fig. 1(a). As can be seen, the signal is really broadband, however, the energy distribution in low frequency is dominate and sharp, which means the low frequency components are under a highly comprehensive amplitude modulation, thereby causing difficulties for accurate feature reconstruction.

Although broadband Lamb wave signal carries rich information of acoustic media, the signal is usually complicated. Narrowband filtering is commonly adopted for signal simplification. As laser inducer signal $s(t)$ is really broadband, to get narrowband responses, the Hanning windowed sinusoid toneburst $f(t)$ is employed as the filter. Thus, the narrowband response resulting from laser source is written as

$$r^m(t) = \int G^m(\omega)F(\omega)\exp(-i\omega t)d\omega, \tag{4}$$

where $F(\omega)$ is the Fourier transform of $f(t)$ and $G^m(\omega)$ is the Fourier transform of $g^m(t)$. Meanwhile, $G^m(\omega)$ is sometimes called transfer function. The example extracted narrow response with 5 cycle center at 50 kHz is shown in Fig. 1(b).

3. Waveform distortion in time domain by amplitude modulation

The response of laser induced signals is under a strong amplitude modulation of system response and attenuation, which will affects both the time duration and time of flight (ToF) of the wave packet. Moreover, for dictionary matching based damage detection method, the neglecting of waveform changes caused by amplitude modulation would result in an inaccurate damage evaluation. The way to

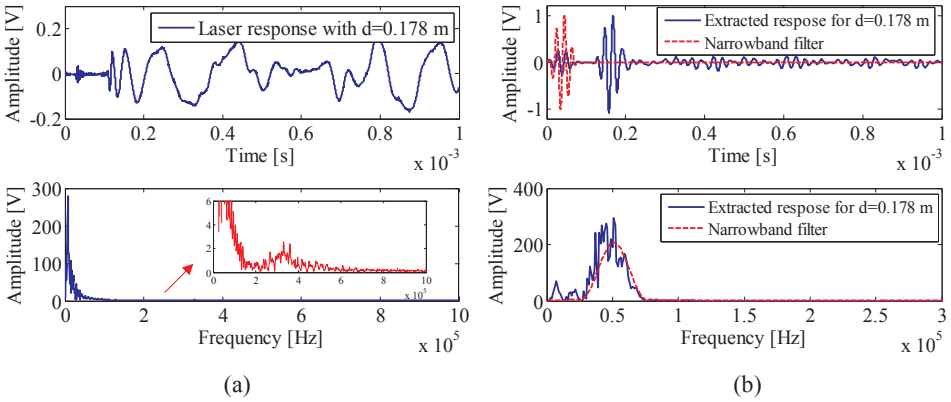

Fig. 1. Example signals from (a) laser source and (b) normalized narrowband extraction.

decompose amplitude modulation and the amplitude modulation influence on waveforms are given in this section.

3.1. Amplitude modulation decomposition

The amplitude response generally consists of two parts: system response and attenuation [11]. Both of them are mode related while the attenuation is distance related. Generally, system response consisting of the whole amplitude modulation parts of the detection system does not rely on propagation distance. Most of time, for a particular detection system, the system response can be treated stably for each mode. In order to build an accurate dictionary for wave propagation model, the amplitude modulation decomposition method for system amplitude and attenuation using multiple received signals is proposed.

Assume that the amplitude response of wave signals with a propagation distance of d is $R(d, \omega)$, then the amplitude item can be simplified by

$$R(d, \omega) = A(\omega)e^{-\alpha(\omega)d}, \tag{5}$$

where $A(\omega)$ is the system amplitude response and $\alpha(\omega)$ is frequency dependent attenuation coefficient. Take the first measurement as the reference and assume that the system response remains stable, the equation (5) can be simplified as

$$B(d_m, \omega) = R(d_m, \omega)/R(d_1, \omega) = e^{-\alpha(\omega)(d_m - d_1)}. \tag{6}$$

With M different measurements, the distances are $d_1,\ldots d_m$. By applying the logarithms to both sides, the Eq. (6) can be rewritten as

$$\ln(\mathbf{B}) = -\boldsymbol{\alpha}\cdot\mathbf{d}. \tag{7}$$

To solve Eq. (6), the least-square method [25] is used. Then, the solution for the attenuation coefficient is given by

$$\boldsymbol{\alpha} = -(\mathbf{d}^T\mathbf{d})^{-1}\mathbf{d}^T\ln(\mathbf{B}). \tag{8}$$

For N total measurements, each time random M sets of data are selected for calculation and then repeat this procedure for K times. Then, the results of attenuation coefficients $\alpha(\omega)$ can be more precise by applying averaging process for $\alpha_k(\omega)$. Furthermore, the system response can be calculated by

$$A(\omega) = \frac{1}{MK}\sum_{k=1}^{K}\sum_{m=1}^{M}[R_k(\mathbf{d}, \omega)/e^{-\alpha_k(\omega)\mathbf{d}}]. \tag{9}$$

Hence, the amplitude modulation of attenuation and system response can be decomposed. Using the experimental data obtained in Section 5, the corresponding attenuation coefficient and system response for A0 mode in this paper can be calculated, which is shown in Fig. 2. In order to avoid the influence of multimode and dispersion, the response amplitude of A0 mode $R(d, \omega)$ is obtained by peak amplitude extraction from various narrowband filtered signals. 7 cycles Hanning windowed sine signals with center frequency ranging from 35 kHz to 180 kHz are adopted as narrowband filter. Fig. 2(a) shows the attenuation coefficient of A0 mode with frequency range from 35 kHz to 180 kHz, while Fig. 2(b) illustrates the source response of A0 mode. As can be seen, the A0 mode signal in low frequency is under a strong amplitude modulation, which may cause a distortion of receiving wave packets.

3.2. The influence of amplitude modulation on time domain signal

Simulated signals are given in this section to show the influence of amplitude modulation on time duration width, ToF delay and the signal difference. The attenuation coefficient and system amplitude response used here are shown in Fig. 2. On the basis of equation (3), A0 mode signals with center frequency of 50 kHz and 3 cycles are simulated as an illustration. Both cases with and without considering amplitude modulation are simulated with propagating distances of 0.2 m, 0.4 m and 0.6 m, which are shown in Fig. 3 (a). Here, t_1 and t_2 are the peak amplitude locations of envelops (ToFs) from the received wave packets with and without amplitude modulation. As can be seen, ToFs for both cases are different. This is reasonable because the spectrum energy distributions are shifted to low frequency shown in Fig. 3(b), which makes the wave packet velocity drop. Hence, the group velocity of the wave packet chosen based on center frequency should be improved.

Time duration of the wave packet is also compared by normalized simulated signals shown in Fig. 3(a). It is obvious that the time duration increases with the deepening of amplitude modulation due to the distance related attenuation. On this basis, it should be noted that the strong amplitude modulation caused by laser detection system and material damping would change the signal a lot, thereby making the prediction of the response signal difficult.

As dictionary based damage detection method, like matching pursuit and sparse reconstruction methods usually employ the simulated signals with different locations as atoms. Here, the correlation coefficients between two cases of simulating signals with and without amplitude considerations are calculated to show the influence of amplitude modulation on atoms changing. As shown in Fig. 4, the signal similarity decreases with the deepening of amplitude modulation. Therefore, to get a more precise matching results, the amplitude considered dictionary should be built as well as the phase considered dictionary.

4. Damage detection through sparse imaging with amplitude modified dictionary

Using sparse reconstruction method to monitor the structural integrity of composite structures is promising, which is based on the reasonable assumption that only few position of structure may exist damages. According to Lamb wave reflection model with amplitude

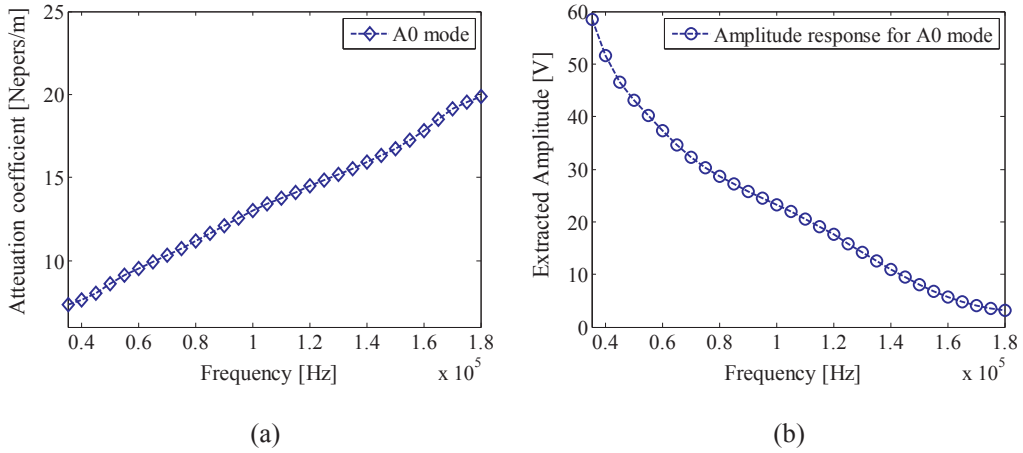

Fig. 2. Attenuation coefficients (a) and amplitude response (b) for A0 mode in low frequency range.

modulation consideration, the new sparse reconstruction method for damage location is proposed.

4.1. Amplitude modified dictionary construction

The general propagation model for Lamb wave is given in Eq. (3). The determination of response relies on the amplitude modulation and the dispersion. Suppose that the source and receiver for the Lamb wave system are located on the structure at $\mathbf{s} = [s_x, s_y]$ and $\mathbf{r} = [r_x, r_y]$. If a damage located at $\mathbf{d} = [d_x, d_y]$, then the distance of the candidate reflections L in the detecting region is given by

$$L = \|\mathbf{d} - \mathbf{r}\|_2 + \|\mathbf{d} - \mathbf{s}\|_2. \tag{10}$$

Ignoring the mode conversion when the Lamb waves encounter the damage, then the damage related dictionary $D(\omega, L)$ for mode m can be expressed as

$$D(\omega, L) = G^m(\omega, L)F(\omega)\exp[ik^m(\omega)L], \tag{11}$$

where $G^m(\omega, L)$ is amplitude modulation coefficient including system response and attenuation for mode m. Based on the amplitude and phase features of Lamb wave propagation, for arbitrary excitation $F(\omega)$ and all possible propagation distance $\mathbf{L}$, then the dictionary $\mathbf{D}$ for the detection system is given by

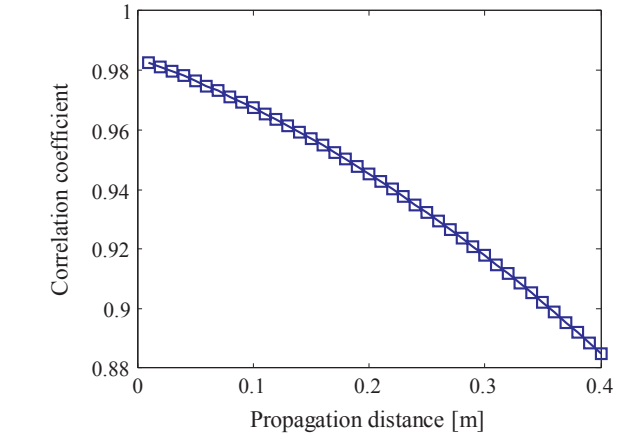

Fig. 4. Signal similarity between simulated signals with and without amplitude modulation.

$$\mathbf{D}^m(\omega, \mathbf{L}) = F(\omega)G^m(\omega, \mathbf{L})\exp[ik^m(\omega)\mathbf{L}]. \tag{12}$$

Therefore, the response of the each possible damage location can be estimated with the consideration of amplitude and phase information.

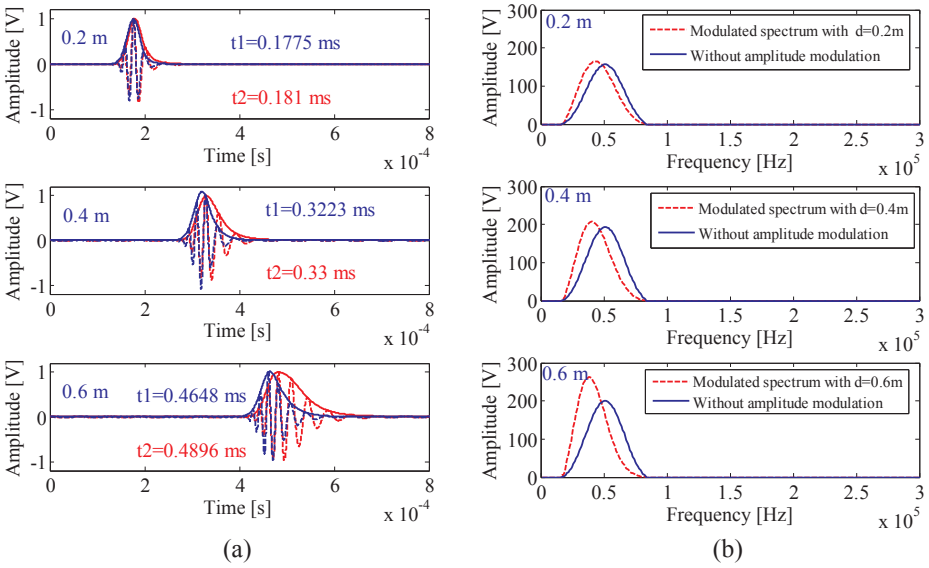

Fig. 3. Normalized simulated signals with and without amplitude modulation in (a) time domain and (b) frequency domain.

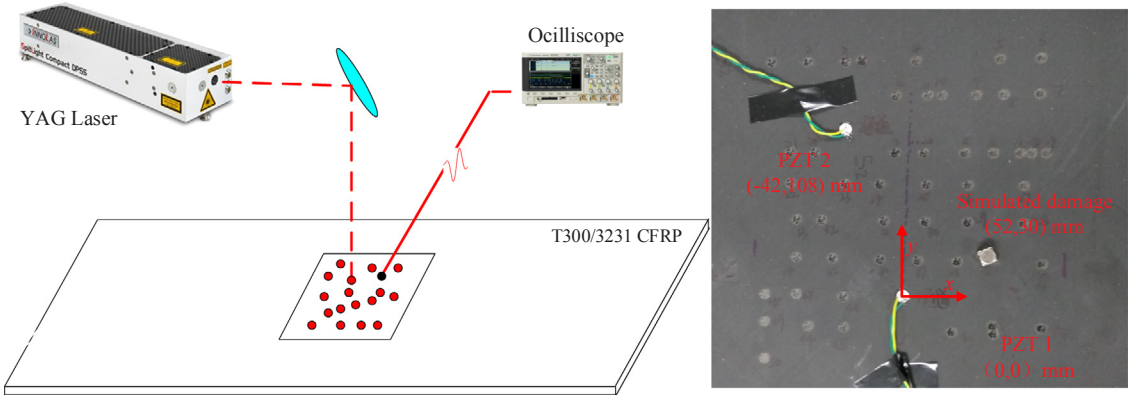

Fig. 5. Scheme diagram of experimental setup.

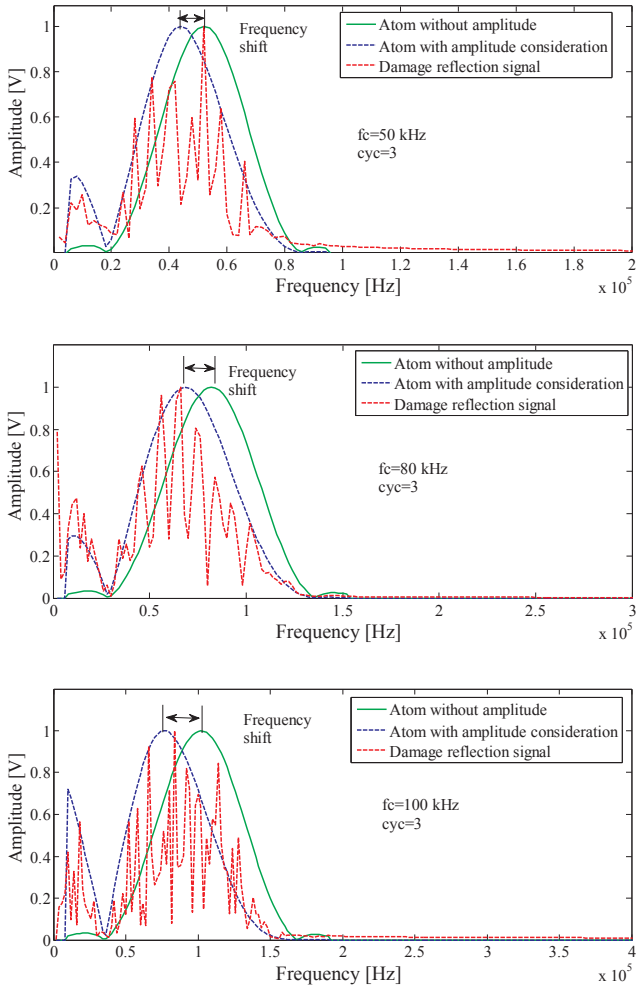

Fig. 6. Amplitude distribution compasion of atoms with response of signal in frequency domain with f_c = 50, 80 and 100 kHz.

4.2. Sparse solution for Lamb wave based damage detection

Suppose that there are M measurements in the detection system and the length of each measurement is N, if the excitation of system is $F(\omega)$, the response of the signals $\mathbf{Y}$ in frequency domain are given by

$$\mathbf{Y} = [y_1\ y_2 \cdots y_M]^{\mathrm{T}}. \tag{13}$$

The location of each pixel in $\mathbf{X}$ represents the possible damage location, if the reflection source exists, then the reflection response signals can be represented as

$$\mathbf{Y} = \mathbf{D}^{\mathrm{T}}\mathbf{X}. \tag{14}$$

$\mathbf{X} = [x_1 \quad x_2 \quad \cdots \quad x_m \quad \cdots \quad x_P]^{\mathrm{T}}$ are the pixel values of the corresponding P grids. As the damages existed in the structure are assumed to be sparse, thereby making the $\mathbf{X}$ sparse which means that most elements in $\mathbf{X}$ are zero.

On the basis of Eq. (12), the dictionary for M measurements becomes a $P \times MN$ matrix $\mathbf{D}$, which is given by

$$\mathbf{D} = [\mathbf{D}_1 \quad \mathbf{D}_2 \quad \cdots \quad \mathbf{D}_{\mathrm{m}} \quad \cdots \quad \mathbf{D}_{\mathrm{M}}]$$

$$= \begin{bmatrix} D_1^1(\omega) & D_1^2(\omega) & \cdots & \\ & D_1^m(\omega) & \cdots & D_1^M(\omega) \\ D_2^1(\omega) & D_2^2(\omega) & \cdots & \\ & D_2^m(\omega) & \cdots & D_2^M(\omega) \\ \vdots & & & \vdots \\ & & & \vdots \\ & & \vdots & \\ D_j^1(\omega) & D_j^2(\omega) & \cdots & \\ & D_j^m(\omega) & \cdots & D_j^M(\omega) \\ \vdots & & & \vdots \\ & & & \vdots \\ & & & \vdots \\ D_P^1(\omega) & D_P^2(\omega) & \cdots & \\ & D_P^m(\omega) & \cdots & D_P^M(\omega) \end{bmatrix} \tag{15}$$

Therefore, the solution of the sparse reconstruction of the damage to the damage detection problem can be set to be [17]

$$\min_{\mathbf{x}} \ \frac{1}{2}\ \|\mathbf{Y} - \mathbf{D}^T\mathbf{X}\|_2^2 + \lambda\ \|\mathbf{X}\|_1, \tag{16}$$

where λ is a denoising parameter that balances sparsity and accuracy [26], in this paper, λ is defined by

$$\lambda = max\ |\mathbf{D}^{\mathrm{T}}\mathbf{Y}|. \tag{17}$$

To solve the sparse reconstruction problem described in Eq. (16), the basis pursuit denoising method [27] is used for calculating. To

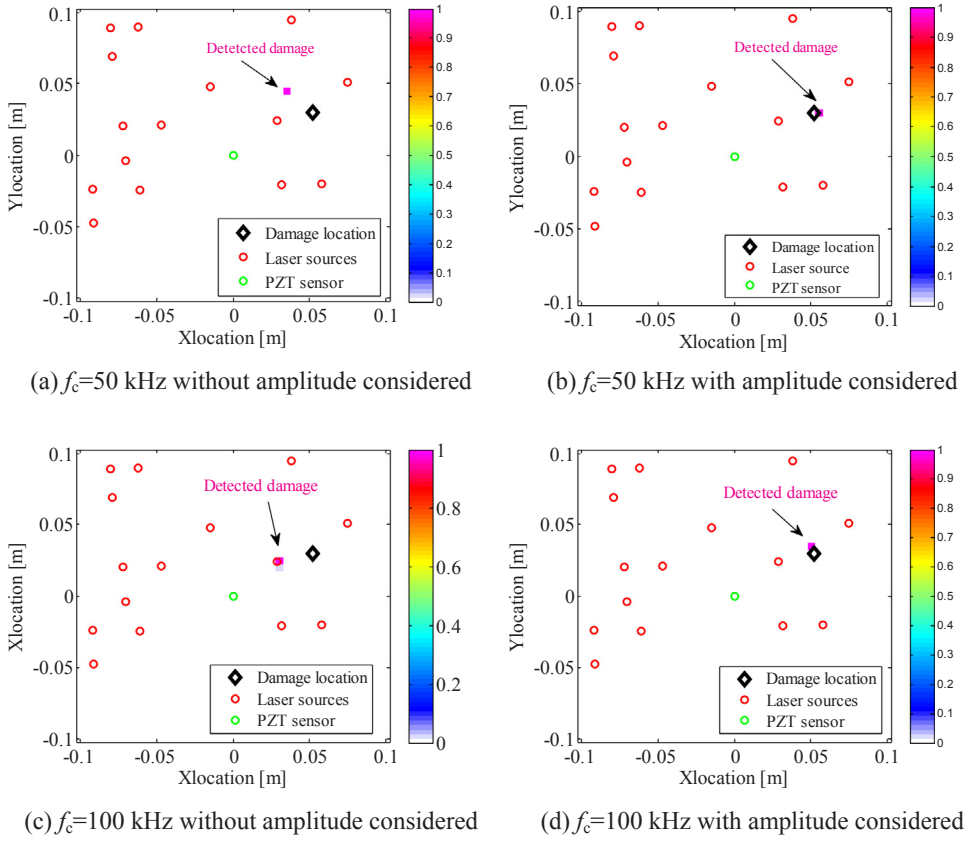

(a) f_c=50 kHz without amplitude considered (b) f_c=50 kHz with amplitude considered

(c) f_c=100 kHz without amplitude considered (d) f_c=100 kHz with amplitude considered

Fig. 7. Damage detection results with 15 sources and λ.

improve the computing efficiency, the Matlab tool package named CVX [28] is used to solve this problem.

5. Experimental investigation

5.1. Experimental setup

The schematic diagram of experimental setup is shown in Fig. 5. The experiment was carried out on a composite plate (CFRP, T300/3231) with a dimension of 700 mm × 700 mm × 2 mm. The layup of composite laminates is $[+45/-45/0/90]_{2s}$ and the thickness of each single laminate is 0.125 mm. A Nd: YAG laser source with a spot size of 6 mm and a wave length of 1064 nm is served as a non-contact actuator. Lamb waves are produced due to the thermoelastic effect and captured by an Agilent oscilloscope. The sampling rate is set to be 10 MHz and 10,000 data points are recoded.

Delamination can be simulated by bonding masses on the surface of laminates for damage detection methods verification [29,30]. In this paper, a square magnet with 10 mm length is attached on both surfaces of the laminates to simulate the damage. The strong suction causes a reflection source of Lamb waves. Two PZTs are bonded on the plate to record signals. The locations of PZT1, PZT2 and damage are (0,0) mm, (−42,108)mm and (52,30)mm, respectively. A hundred of measurements are obtained by two PZT sensors in total. However, to verify the proposed method, only few measurements are selected randomly to use.

5.2. Efficiency verification for amplitude modified dictionary

Besides the high sensitivity of A0 mode to the damage, the A0 mode is chosen for method verification due to the following consideration. A0 mode is dominate in low frequency and the propagation of A0 mode is almost isotropic. The direction difference of the wave propagation is ignored due to the quasi-isotropy assumption of the laminates which is verified through theoretical calculations. In addition, the A0 mode is under the strong amplitude modulation in low frequency, which should be valued. The narrowband signals are extracted to verify the method. In order to guarantee the SNR of the extracted signals, the narrowband filter should be below 180 kHz. The toneburst signal with 3 cycles centered at 50 kHz, 80 kHz and 100 kHz where A0 mode is dominate are adopted for narrowband filters. The normalized differential signals resulting from the subtraction of damage signals and baseline signals are used for further analysis in frequency domain.

Signal distortion in frequency domain (including frequency center and frequency bandwidth) are amplitude related. As shown in Fig. 6, example signals with different centered frequency recorded from the laser source located at (−0.01, 0.13) mm are presented. It can be seen that the amplitude distribution of reflections from damage agrees well with that of amplitude considered atoms. However, the frequency shift of given example signals compared with only phase considered atoms are 6 kHz, 10 kHz and 28 kHz. Hence, the distribution results of frequency spectrum demonstrate the necessity of amplitude correction for dictionary construction. As the inherent reason of dictionary is using the atoms to match the signals, the more accurate the atoms, the more accurate the detection results will be.

5.3. Damage detection results and discussion

Although there are 100 source points in total, only some random sources are used for method verification. The results with different sources and λ are given to show the improvement of the algorithm. Here, λ is determined empirically under the consideration of sparsity and accuracy. Based on the previous experiment, the sparsity coefficient λ is specified to be $\lambda = \max|A^T y|$.

First of all, the detection results with and without amplitude consideration are compared in Fig. 7. Here, the source number is set to be 15 and the denosing parameter is given by λ. The location of laser

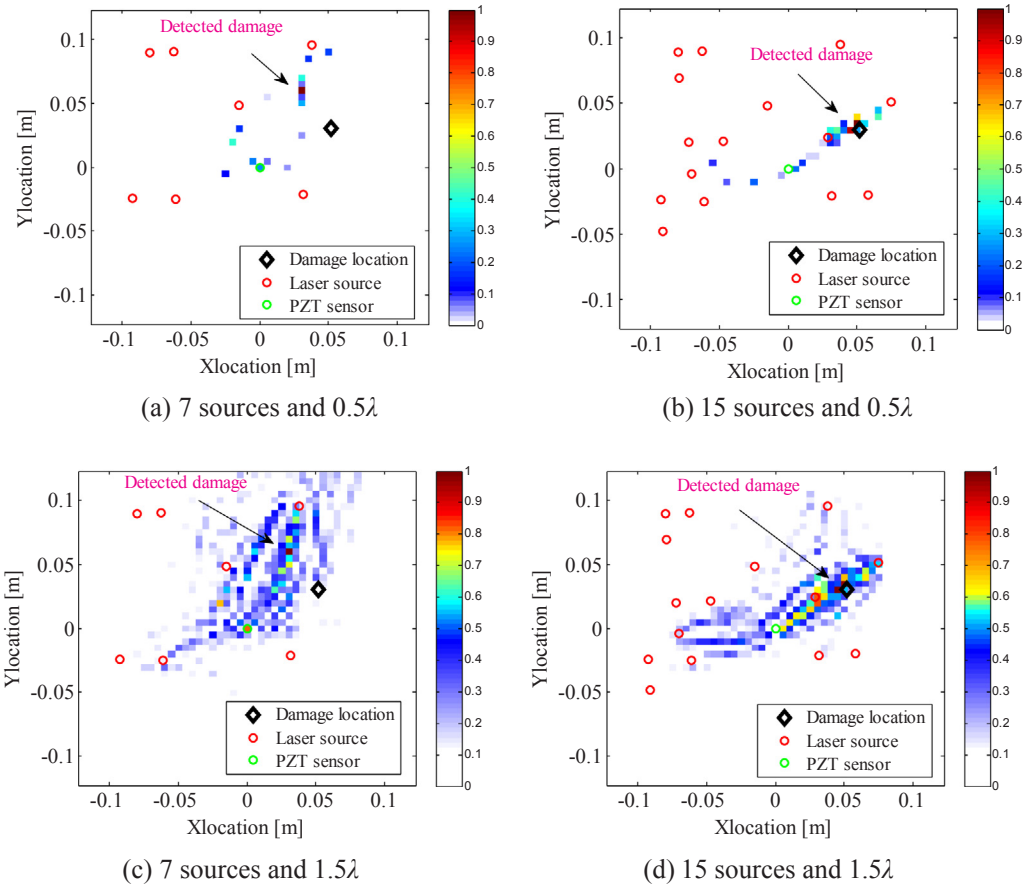

Fig. 8. Performance of sparse imaging with various input parameters.

sources are selected randomly from the signals recorded by PZT1. The parameters of narrowband filter are 50 kHz and 100 kHz with 3 cycles. It can be seen that, the damage detection results are with high accuracy when using the amplitude considered atoms proposed in this paper. Meanwhile, the results with the given parameters have an extremely high SNR.

Secondly, the detection results with different input parameters including numbers of sources and denoising parameters are compared. The denoising parameter set to be 0.5 λ and 1.5 λ together with the source number of 7 and 15 are investigated. The narrowband filter with 100 kHz centered frequency and 3cycles is used. The improved dictionary is adopted for calculation. The results with source numbers of 7 and 15 are given in Fig. 8. It can be concluded that the denosing parameter λ determines the SNR of the final result. The bigger deviation of the denoising parameter λ, the lower the SNR will be. Additionally, the larger the source number, the more accurate the results will be. This is reasonable due to the more damage feature information will be inputted to the sparse reconstruction algorithm. The more sources will also decrease the measurement error including phase and amplitude. Therefore, the best sparsity coefficient at these images is $\lambda = \lambda_{max}$ and the number of laser sources also affect the performance of sparse imaging.

6. Conclusions

In this paper, an amplitude modified sparse imaging method is proposed to locate the damages in composite laminates. The strong comprehensive amplitude modulation effect for non-contact laser induced Lamb waves in viscoelastic composite plates has a great influence on dictionary reconstruction when using sparse method for damage detection. Hence, the dictionary with a comprehensive consideration of phase and amplitude is built for sparse imaging. Then, the sparse solution using frequency domain signals is proposed. The experimental results show the good performance of sparse imaging method for damage detection using improved dictionary. As a result, the damage can be detected with high accuracy. Some conclusions are listed below.

1. The system response including laser source thermoelastic coefficient, sensor mechanical-electro coefficient, and mode excitability together with the distance related attenuation cause a strong amplitude modulation in low frequency, thereby making signal changes both in time domain and frequency domain.
2. Both amplitude and phase considered dictionary can be more suitable for sparse reconstruction method for damage detection, which will make the detection results more accurate.
3. The performance of sparse imaging method relies on the denosing parameters and numbers of sources.

Acknowledgement

The work is supported by the National Natural Science Foundation of China [grant number 51505365, 51421004], and the Open Foundation of Henan Key Laboratory of Underwater Intelligent Equipment (grant number KL03A1804), and the China Scholarship Council (CSC), which are highly appreciated by the authors.

References

[1] A.K. Kaw, Mechanics of Composite Materials, CRC Press, 2005.
[2] S.H.D. Valdes, C. Soutis, Delamination detection in composite laminates from variations of their modal characteristics, J. Sound Vib. 228 (2000) 1–9.
[3] Z. Su, L. Ye, Identification of Damage Using Lamb Waves, Springer, London, 2009.
[4] A.K. Mal, Impact of damage on propagation of Lamb waves in plates, Proceedings of

SPIE - The International Society for, Opt. Eng. 137 (1999) 503–508.
[5] C.T. Ng, M. Veidt, A Lamb-wave-based technique for damage detection in composite laminates, Smart Mater. Struct. 18 (2009) 074006.
[6] Z. Su, L. Ye, X. Bu, A damage identification technique for CF/EP composite laminates using distributed piezoelectric transducers, Compos. Struct. 57 (2002) 465–471.
[7] R. Murayama, Study of driving mechanism on electromagnetic acoustic transducer for Lamb wave using magnetostrictive effect and application in drawability evaluation of thin steel sheets, Ultrasonics 37 (1999) 31–38.
[8] H. Kim, K. Jhang, M. Shin, J. Kim, A noncontact NDE method using a laser generated focused-Lamb wave with enhanced defect-detection ability and spatial resolution, NDT E Int. 39 (2006) 312–319.
[9] J.C. Cheng, S.Y. Zhang, Quantitative theory for laser-generated Lamb waves in orthotropic thin plates, Appl. Phys. Lett. 74 (1999) 2087–2089.
[10] T.T. Wu, Y.H. Liu, On the measurement of anisotropic elastic constants of fiber-reinforced composite plate using ultrasonic bulk wave and laser generated Lamb wave, Ultrasonics 37 (1999) 405–412.
[11] J. Lin, F. Gao, Z. Luo, L. Zeng, High-resolution lamb wave inspection in viscoelastic composite laminates, IEEE Trans. Ind. Electron. 63 (2016) 6989–6998.
[12] J.S. Hall, J.E. Michaels, Minimum variance ultrasonic imaging applied to an in situ sparse guided wave array, IEEE Trans. Ultrason. Ferroelectr. Freq. Control 57 (2010) 2311–2323.
[13] S.M. Prasad, R. Jagannathan, K. Balasubramaniam, C.V. Krishnamurthy, structural health monitoring of anisotropic layered composite plates using guided ultrasonic lamb wave data, 2004, pp. 1460–1467.
[14] J. Hua, J. Lin, L. Zeng, High-resolution damage detection based on local signal difference coefficient model, Struct. Health Monit. 14 (2015) 20–34.
[15] R.M. Levine, J.E. Michaels, Block-sparse reconstruction and imaging for Lamb wave structural health monitoring, IEEE Trans. Ultrason. Ferroelectr. Freq. Control 61 (2014) 1006–1015.
[16] S.G. Mallat, Z. Zhang, Matching pursuits with time-frequency dictionaries, IEEE Trans. Signal Process. 41 (1993) 3397–3415.
[17] R.M. Levine, J.E. Michaels, Model-based imaging of damage with Lamb waves via sparse reconstruction, J. Acoust. Soc. Am. 133 (2013) 1525–1534.
[18] M.L. De, M. Ruzzene, B. Xu, E. Baravelli, N. Speciale, Warped basis pursuit for damage detection using lamb waves, IEEE Trans. Ultrason. Ferroelectr. Freq. Control 57 (2010) 2734.
[19] J.L. Rose, Ultrasonic Guided Waves in Solid Media, Cambridge University Press, 2014.
[20] S. Pant, J. Laliberte, M. Martinez, B. Rocha, Derivation and experimental validation of Lamb wave equations for an n-layered anisotropic composite laminate, Compos. Struct. 111 (2014) 566–579.
[21] M.J.S. Lowe, Matrix techniques for modeling ultrasonic waves in multilayered media, IEEE Trans. Ultrason. Ferroelectr. Freq. Control 42 (1995) 525–542.
[22] P.D. Wilcox, A rapid signal processing technique to remove the effect of dispersion from guided wave signals, IEEE Trans. Ultrason. Ferroelectr. Freq. Control 50 (2003) 419.
[23] B. Xu, Z. Shen, J. Wang, X. Ni, J. Guan, J. Lu, Thermoelastic finite element modeling of laser generation ultrasound, J. Appl. Phys. 99 (2006) 3559.
[24] F. Bruno, J. Laurent, P. Jehanno, D. Royer, C. Prada, Laser beam shaping for enhanced Zero-Group Velocity Lamb modes generation, J. Acoust. Soc. Am. 140 (2016) 2829.
[25] A.D. Puckett, M.L. Peterson, A semi-analytical model for predicting multiple propagating axially symmetric modes in cylindrical waveguides, Ultrasonics 43 (2005) 197–207.
[26] K. Koh, S.J. Kim, S. Boyd, An interior-point method for large-scale l 1 -regularized logistic regression, IEEE J. Sel. Top. Signal Process. 1 (2008) 606–617.
[27] S.S. Chen, D.L. Donoho, M.A. Saunders, Atomic decomposition by basis pursuit, SIAM Rev. 43 (2001) 129–159.
[28] M. Grant, S. Boyd, Y. Ye, Disciplined convex programming, Nonconvex Optim. Appl. 84 (2007) 155–210.
[29] H. Sohn, G. Park, J.R. Wait, N.P. Limback, C.R. Farrar, Wavelet-based active sensing for delamination detection in composite structures, Smart Mater. Struct. 13 (2003) 153.
[30] J.B. Ihn, F.K. Chang, Pitch-catch active sensing methods in structural health monitoring for aircraft structures, Struct. Health Monit. 7 (2008) 5–19.